Quasiclassical Trajectory Calculation of the Reaction O (^3P)+HI→OH (X)+I

Nishiyama, Nobuaki
(Present abbress)The Center of Advanced Instrumental Analysis

Sekiya, Hiroshi
Institute of Advanced Material Study Kyushu University

Nishimura, Yukio
Institute of Advanced Material Study Kyushu University

https://doi.org/10.15017/6524

出版情報：九州大学機能物質科学研究所報告. 2 (1), pp.29-34, 1988-06-30. 九州大学機能物質科学研究所
バージョン：
権利関係：

Rep. Inst. Advanced Material
Study, Vol. 2, No. 1, 29-34
(1988. 6)

Quasiclassical Trajectory Calculation of the Reaction O (^{3}P)+HI→OH (X)+I

Nobuaki NISHIYAMA*, Hiroshi SEKIYA and Yukio NISHIMURA

Dedicated to Professor Otohiko Tsuge on the occasion of his retirement

Three-dimensional quasiclassical trajectory calculations have been performed for the O(^3P)+HI/DI⟶OH(X)/OD(X)+I reactions by using generalized LEPS potential energy surfaces. The calculated vibrational state distribution of OH is in good agreement with the experimental one. The vibrational excitation of OH has been ascribed to the **H+LH′** mass effect on the highly repulsive potential energy surface, while the effect of the secondary encounters on the product vibrational energy disposal is small.

In recent years, hydrogen transfer reactions have been of considerable interest as a prototype of the **H+LH′** (**H** and **H′**: heavy atom, **L**: ligth atom) reactions. In general, reactions with the **H+LH′** mass combination are known to exhibit high degree of product internal excitation on repulsive surfaces. In previous paper,[1] we reported the vibrational energy distribution of CH resulting from the C(^3P)+HI reaction. The reaction dynamics of the O(^3P)+HI reaction is expected to be similar to that of the C(^3P)+HI reaction due to the mass dependent effect. However, the vibrational distribution of OH differs significantly from that of CH.[2] The fraction of the available energy deposited in vibration $< f_v >_{OH}$ and $< f_v >_{CH}$ were measured to be 0.67 and 0.31, respectively.

Very recently,[3] we carried out three dimensional quasiclassical trajectory calculation for the C(^3P)+HI reaction. In the present work, trajectory calculations for the O(^3P)+HI reaction have been performed and compared with the calculated results for the C(^3P)+HI reaction in order to elucidate the difference between $< f_v >_{OH}$ and $< f_v >_{CH}$. A similar study has been reported on the trajectory calculations for the O(^3P)+HI reaction by Persky and Broida,[4] when our work was completed. However, their calculations were not focused on effect of secondary encounters due to the **H+LH′** mass combination on the product vibrational distribution. In this study, we have quantitatively investigated the difference between the O(^3P) and C(^3P)+HI reactions by counting secondary encounters.

Received February 25, 1988

*Present abbress: The Center of Advanced Instrumental Analysis.

Computation methods

In this work, trajectory calculations were performed by using semiempirical London-Eyring-Polanyi-Sato (LEPS) potential energy surface with three Sato parameters.[5] Preliminary trajectory calculations were carried out for a large number of the LEPS potential energy surfaces. The surface that is in best agreement with experimental kinetic data was used to calculate the product vibrational energy distribution. The Morse and Sato parameters for the selected surface are presented in Table 1. A contour diagram of this surface for collinear configuration is given in Fig. 1. The saddle point for the collinear configuration is located at the point of the interatomic distances: (r_{OH}=1.85 Å, r_{HI} =1.61 Å), and the barrier height is 0.63 kcal/mol. The classical equations of motion were integrated by means of Runge-Kutta-Verner method[6] with a variable step size. Trajectories were calculated for the initial HI vibrational-rotational states v=0 and J=0, ..., 7. The initial collisional energy was estimated to be 0.6 kcal/mol by using the most probable relative collision velocity at 300 K.[7] The collision shell radius ρ_0 required for determining the initial separation of O atom and HI molecule was taken as 6.0 Å. The remaining conditions (the impact parameter, the three orientation angles and the vibrational phase of

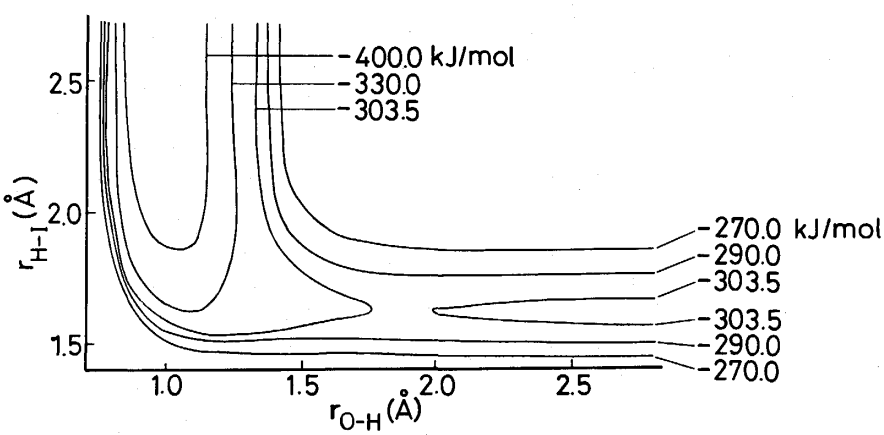

Fig. 1 A contour diagram of the selected surface for collinear configuration.

Table 1. Parameters for LEPS surfaces of OHI.

Fragment	β_e(Å)	r_e(Å)	D_e(kJ/mol)	Sato parameter
OH	2.295	0.970	445.36	0.135
OI	2.566	1.868	177.83	− 0.020
HI	1.752	1.609	306.00	0.075

Table 2. Influence of HI rotational excitation on reactivity

J	E_r(kcal/mol)	S_r(Å²)
0	0.00	n.r.[a]
1	0.04	n.r.
2	0.11	n.r.
3	0.22	0.038
4	0.36	0.105
5	0.54	0.248
6	0.76	0.377
7	1.02	0.459

a) No reactive collision for 1000 collisions.

the HI molecule) were selected using a Monte Carlo procedure. The maximam impact parameter was taken as 3.0 Å. The initial and final rovibrational states of diatomic molecules were dealt with a quasiquantization method proposed by Truhlar et al.[8]

Results and Discussion

A. Effect of the HI rotational excitation on the reaction cross section

In this work, a large number (8200) of trajectories were calculated. The data were averaged over the initial HI rotational states (J=0,..., 7) with weights corresponding to a temperature at 300 K.

In Table 2 is shown the dependence of the cross section on the initial rotational state of HI. It is found that reactivity increases monotonously with J. Persky and Broida [9][10] carried out the trajectory calculations for the $O(^3P)$+HCl, HBr reactions. They found that the cross sections increase markedly with the HX rotational quantum number. This observation was interpreted as due to "energy effect", which means that rotational energy would be available for reaction through vibrational-rotational interaction. In the $O(^3P)$+HI reaction, a similar dependence of the cross section on the initial rotational state has been obtained, suggesting that the three reactions proceed on similar repulsive potential energy surfaces.

Table 3. Calculated vibrational distribution of OH(X) resulting from the $O(^3P)$ + HI reaction.

	v = 0	v = 1	v = 2	v = 3	$\langle f_v \rangle_{OH}$
Calc. (this work)	0.00	0.03	0.25	0.72	0.75
Calc. (Persky[a])	0.00	0.03	0.33	0.64	0.73
Exp.[b]	0.02	0.11	0.36	0.51	0.67

a) ref. 4 b) ref. 2

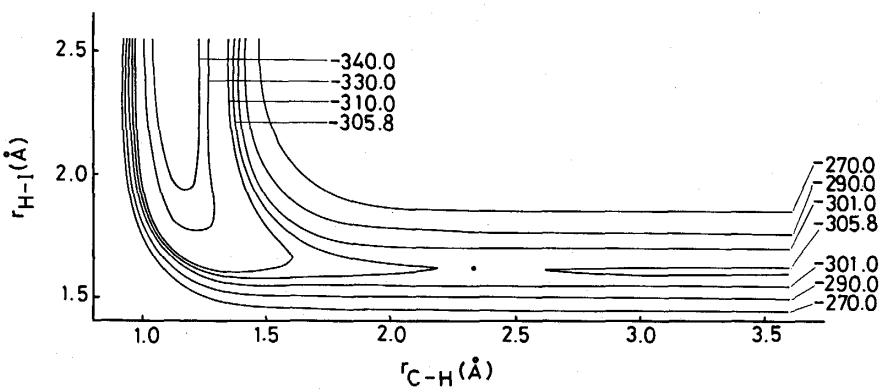

Fig. 2 A contour diagram for collinear configuration of the $C(^3P)$+HI reaction. The saddle point is indicated as the closed circle. The energy barrier higth is 0.06 kcal/mol.

B. Vibrational state distribution of the product OH

The calculated OH vibrational state distribution is shown in Table 3 together with the experimental distribution. In addition, the calculated results by Persky and Broida [4] are also shown in Table 3. It should be noted that the calculated distribution agrees well with the experimental one.

The $O(^3P)$+HI reaction has a similar mass-combination to the $C(^3P)$+HI. Both reactions are expected to have the similar vibrational energy disposal. However, very large difference is seen in the values of the product $< f_v >$ between the $C(^3P)$+HI and $O(^3P)$+HI reactions ($< f_v >_{CH}=0.31$, $< f_v >_{OH}=0.69$). Very recently,[3] we carried out the trajectory calculation for the $C(^3P)$+HI reaction by using a procedure similar to the present work. In Fig. 2 is shown a contour diagram for collinear configuration of the $C(^3P)$+HI reaction system. It is found

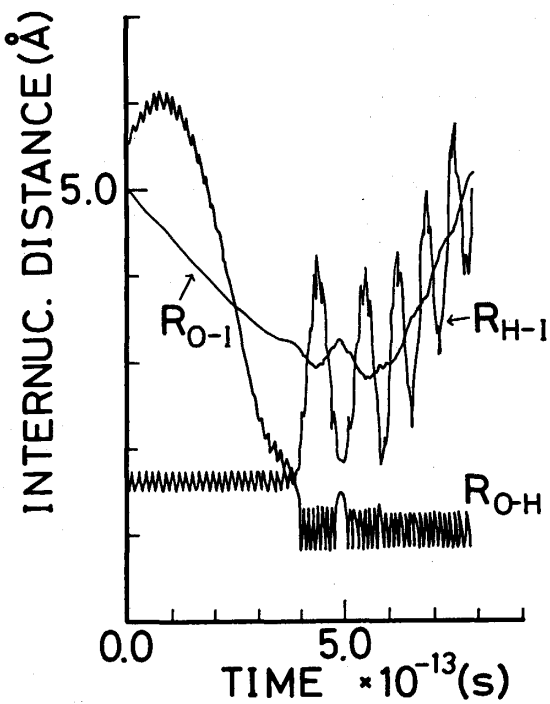

Fig. 3 Plots of internuclear distances for the three atoms during the course of the typical secondary encounter.

Table 4. Classification of secondary encounters for the $O(^3P)$ and $C(^3P)$ + HI reactions.

Reaction	N_r / N total	Secondary encounter
O + HI	94 / 1200	4 / 94 secondary encounters
C + HI	67 / 730	11 / 67 secondary encounters

In the case of the $C(^3P)$ + HI reaction, the calculations were performed by using the surface of single Sato parameter 0.23 and the initial vibrational-rotational states of HI were v = 0 and J = 1. In the $O(^3P)$ + HI reaction, the initial vibrational-rotational states of HI were v = 0 and J = 5.

Table 5. Isotope effect on the vibrational distributions of OH(X) and CH(X) resulting from the O(^3P) and C(^3P) + HI reactions, respectively.

Reaction	v = 0	v = 1	v = 2	v = 3	v = 4	$\langle f_v \rangle$
O + HI	0.00	0.03	0.29	0.67		0.72
O + DI	0.00	0.00	0.03	0.45	0.52	0.70
C + HI[a)]	0.44	0.56				0.39
C + DI[a)]	0.19	0.56	0.25			0.55

In the case of the C(^3P) + HI reaction, the calculations were performed by using the surface of single Sato parameter 0.25 and the initial vibrational-rotational states of HI were v = 0 and J = 1. For the O(^3P) + HI reaction, the initial vibrational-rotational states of HI were v = 0 and J = 5.

that the surface for the C(^3P)+HI reaction is more attractive relative to that for the O(^3P)+HI reaction. The results for the C(^3P)+HI reaction suggested that enhanced secondary encounters on attractive energy surface invoked a decrease in the vibrational excitation of the product CH. In Table 4 is shown counting of the secondary encounter classification from all calculated trajectories together with the results of the C(^3P)+HI reaction. In Fig. 3 are shown plots of internuclear distances for the three atoms during the course of the typical secondary encounter. It is generally acknowledged that the secondary encounter is due to heavy-light-heavy mass combination, and is enhanced on more attractive potential energy surface. As shown in Fig. 3, the secondary encounter lowers the amplitude of the new O–H bond oscillation. Only a few secondary encounters occur in the O(^3P)+HI reaction in contrast with the C(^3P)+HI reaction, as shown in Table 4. The effect of the secondary encounter on the product vibrational energy distribution is insignificant in the O(^3P)+HI reaction. We investigated isotope effect on the product vibrational energy disposal for the O+HI/DI reactions. The calculated result is presented in Table 5 together with that for the C(^3P)+HI reaction. In contrast with the C(^3P)+HI reaction, no isotope effect on the vibrational energy disposal is seen in the O(^3P)+HI reaction. In general, the secondary encounter is enhanced owing to a faster moving hydrogen atom between the more massive atoms. No isotope effect on the vibrational energy disposal also supports that the secondary encounter is insignificant in the O(^3P)+HI reaction system. Accordingly, the lowering of the product vibrational excitation due to the secondary encounter would not occur on the highly repulsive potential energy surface in the O(^3P)+HI reaction system.

In summary, the difference of the product vibrational energy disposal between the O(^3P)+HI and C(^3P)+HI reactions is responsible for the difference in the features of potential energy surface. Since the potential energy surface for the O(^3P)+HI reaction system is of highly repulsive character, the possibility of the secondary encounter is small. Thus, the vibrational excitation of the product OH(X) is due to the H+LH′ mass effect on the highly repulsive potential energy surface.

References

1) N. Nishiyama, H. Sekiya and Y. Nishimura, J. Chem. Phys., **84,** 5213 (1986).
2) B. S. Agrawalla, A. S. Manocha and D. W. Setser, J. Phys. Chem., **85,** 2873 (1981).
3) N. Nishiyama, H. Sekiya and Y. Nishimura, Chem. Phys., **123,** 359 (1988).
4) A. Persky and M. Broida, Chem. Phys., 114, **85** (1987).
5) P. J. Kuntz, E. M. Nemeth, J. C. Polanyi, S. D. Rosner and C. E. Young, J. Chem. Phys, **44,** 1168 (1966).
6) J. H. Verner, SIAM J. Numer. Anal., **15,** 772 (1978).
7) S. Golden, Elements of the Theory of Gases (Addison-Wesley, 1964).
8) D. G. Truhlar and J. T. Muckerman, Atom-Molecule Collision Theory: A Guide for the Experimentalist (R. B. Bernstein ed.) (Plenum Press, New York, 1979) p.505.
9) A. Persky and M. Broida, J. Chem. Phys., **81,** 4352 (1984).
10) M. Broida, M. Tamir and A. Persky, Chem. Phys., **110,** 83 (1986).